



HAL
open science

Degradation of historical paper induced by synchrotron X-ray technical examination

Alice Gimat, Sebastian Schöder, Mathieu Thoury, Anne Laurence Dupont

► **To cite this version:**

Alice Gimat, Sebastian Schöder, Mathieu Thoury, Anne Laurence Dupont. Degradation of historical paper induced by synchrotron X-ray technical examination. *Cellulose*, 2022, 29 (8), pp.4347-4364. 10.1007/s10570-022-04552-3 . hal-03772595

HAL Id: hal-03772595

<https://hal.science/hal-03772595>

Submitted on 4 Oct 2022

HAL is a multi-disciplinary open access archive for the deposit and dissemination of scientific research documents, whether they are published or not. The documents may come from teaching and research institutions in France or abroad, or from public or private research centers.

L'archive ouverte pluridisciplinaire **HAL**, est destinée au dépôt et à la diffusion de documents scientifiques de niveau recherche, publiés ou non, émanant des établissements d'enseignement et de recherche français ou étrangers, des laboratoires publics ou privés.

Copyright

Degradation of historical paper induced by synchrotron X-ray technical examination

Alice Gimat^{1*}, Sebastian Schöder², Mathieu Thoury³, Anne-Laurence Dupont^{1*}

¹ *Centre de Recherche sur la Conservation des Collections (CRC, CNRS UAR 3224), Muséum National d'Histoire Naturelle, 36 rue Geoffroy St Hilaire 75005 Paris, France*

² *Synchrotron SOLEIL, 91192 Gif-sur-Yvette, France;*

³ *IPANEMA, CNRS, Ministère de la Culture, UVSQ, USR3461, Université Paris Saclay, 91192 Gif-sur-Yvette, France;*

**corresponding authors: alice.gimat@mnhn.fr and anne-laurence.dupont@mnhn.fr*

Keywords. calcium carbonate, cellulose degree of polymerization, gelatin, iron gallate ink, yellowing, UV fluorescence.

Abstract

This research explores how intrinsic factors such as constituents and degradation state can impact the modifications incurred in aged papers during and after X-ray examination. To this end laboratory model papers, artificially aged, and 18th and 19th century archival documents, with and without additives (gelatin, calcium carbonate) and iron gallate ink, were exposed to Synchrotron X-ray radiation at doses commonly applied (7 Gy to 4 kGy). The threshold dose of 210 Gy previously shown to incur damage in unaged cotton papers falls in this range. Glycosidic scissions, hydroxyl free radicals, UV luminescence and yellowing were measured immediately after the irradiation, and were monitored over a period of three years. Cellulose depolymerization was lower in the aged papers, as well as in the papers containing calcium carbonate and gelatin, than in the unaged fully cellulosic papers. Compared to the papers with no additives, there were more hydroxyl free radicals in the papers with calcium carbonate and slightly less in the gelatin sized papers. UV luminescence and yellowing both appeared post-irradiation, with a delay of several weeks to months. The papers with iron gallate ink showed limited degradation in the low doses range, most probably due to recombination of the free radicals produced. Doses below 4 kGy did not cause yellowing or UV luminescence of the archival papers within the whole monitoring period. The archival papers in good conservation state depolymerized to the same extent as the model papers, while the most degraded archival papers were less impacted than the latter.

Introduction

Because they are perceived as non-destructive, X-ray analytical techniques are commonly used to examine historic documents and artworks on paper and gain insight into their materials,

32 manufacturing techniques and history (Creagh 2007; Albertin et al. 2015; IAEA 2016; Kozachuk
33 et al. 2016; Pouyet et al. 2017). Because they are ionizing, X-rays induce changes in organic (as
34 well as inorganic) materials, yet the potential damage to the artefacts is never considered. This is
35 largely due to the fact that very little is known about the degradation incurred and the reactions
36 involved. This lack of knowledge and awareness underlines the need to investigate the issue.

37 Among the few studies that tackle with this problem, some have shown cellulose depolymerization,
38 oxidation and changes in the optical properties under X-ray exposures (Mantler and Klikovits 2004;
39 Kozachuk et al. 2016; Gimat et al. 2020) as well as during yet gamma-ray irradiation (shorter
40 wavelengths than X-rays) used for mold disinfection (Ershov 1998; Bouchard et al. 2006; Henniges
41 et al. 2013; Bicchieri et al. 2016) . Our recent results have shown that in quasi-pure cellulose paper,
42 the impact of X-rays was proportional to the dose (Gimat et al. 2020). Due to the large diversity in
43 the components and in the degradation state of historic cellulosic artefacts, the global impact of X-
44 ray photons is however difficult to foresee, hence the rationale for the present study.

45 Paper is made of plant fibers, which besides cellulose, most often also contain other biopolymers
46 such as hemicelluloses and lignin. Additives, fillers and sizing, are usually added to writing and
47 drawing quality papers to enhance usability parameters: e.g. reduce water permeability, increase
48 opacity and enhance brightness. In cultural heritage collections, such papers also often bear media
49 such as inks and pigments. The materials and chemicals used are diverse. In ambient conservation
50 conditions, a number of these additives can impact the paper degradation rate. For instance gelatin
51 (Dupont 2003a) and alkaline minerals (Reissland 1999; Sequeira et al. 2006; Ahn et al. 2012; Poggi
52 et al. 2016) have been shown to decrease the cellulose depolymerization rate, whereas transition
53 metals in inks and pigments promote degradation by producing acids and free radicals (Selih et al.
54 2007; Potthast et al. 2008). If and how additives can impact the radiation-induced degradation of
55 cellulosic paper is still unknown. The presence of absorbing elements, such as iron in the metal-
56 gallate ink or calcium in the fillers could have a shielding effect and decrease the nominal X-ray
57 dose, thereby lowering the degradation impact. Such a shielding effect could also be counteracted
58 by the free radicals formed via the transition metals, which are known cellulose degradation
59 promoters (Emery and Schroeder 1974; Jeong et al. 2014). It has been shown that iron-containing
60 pigments undergo a redox reaction under X-ray radiation (Bertrand et al. 2015; Gervais et al. 2015;
61 Gimat 2016). Moreover, the structural modification of an additive under irradiation can also affect
62 the paper degradation rate. For instance, X-rays were shown to produce defects inside calcium

63 carbonate (Kabacińska et al. 2017), whereas polypeptide chains (e.g. gelatin) were shown to
64 undergo hydrolysis (Moini et al. 2014). Bicchieri et al. have examined the combined impact of the
65 degradation state and certain paper additives on the degradation incurred by ionizing radiation used
66 for mold disinfection (Bicchieri et al. 2016). The authors used gamma-rays at a dose of 3 kGy.
67 They tested cellulose paper Whatman n°1, as well as a commercial permanent paper (with CaCO₃
68 filler and optical brighteners, and sized with alkyl ketene dimers), which they pre-degraded by an
69 acid treatment. The acid treated samples showed less radiation induced depolymerization than the
70 Control samples, indicating that the degradation state played a role. The permanent paper yellowed
71 more than Whatman n°1, which was attributed to structural modifications of calcium carbonate and
72 optical brighteners under gamma radiation. To our knowledge, such study has not been conducted
73 using X-rays, nor at lower doses used during synchrotron X-ray examination of cellulosic cultural
74 heritage artefacts. This lack of research motivated the present study, which attempts at better
75 understanding the mitigated impact of X-rays on paper, depending on the fiber deterioration level
76 and on the presence of components other than the fibers.

77 Handmade linen rag papers from the 18th and 19th century and industrially-made cotton linters
78 papers (Whatman n°1) to which various additives were incorporated (gelatin, calcium carbonate
79 and iron gallate ink) were exposed to synchrotron X-ray radiation. The aim was (i) to study the
80 impact of the photon energy and (ii) reach high doses, similar to those used during spectroscopic
81 examinations with instruments in such large-scale facilities. The papers, some of which had been
82 previously artificially aged, were irradiated at doses in the range 0.007-4 kGy. The samples were
83 characterized immediately after the exposure using a multiscale analytical procedure developed in
84 a previous study (Gimat et al. 2020), which encompasses the macroscopic (yellowing and UV
85 luminescence) and the microscopic scales (glycosidic scissions and formation of hydroxyl
86 radicals). The changes were monitored over a period of three years.

87

88 **Materials and Methods**

89 **Paper samples**

90 *Laboratory-prepared samples*

91 Two types of paper were used: Whatman n°1 (W), which is a commercial paper made of cotton
92 linters (min. 98% alpha cellulose), and a linen rag paper (R) manufactured using traditional stamper
93 beating at Moulin du Verger papermill (Puymoyen, France). W and R were used either with no
94 further modification (Control samples), or upon undergoing various artificial aging treatments
95 (aged samples), in an attempt to approach the molecular degradation state of centuries old cultural
96 heritage papers. Two artificial aging conditions, one predominantly hygrothermal (*hyg*) and the
97 other predominantly oxidative (*ox*), were used to depolymerize and increase the carbonyl content
98 of cellulose. The conditions were adjusted so as to achieve a similar degree of polymerization (*DP*)
99 and a different degree of oxidation in the *hyg* and *ox* samples.

100 *Hyg* aging of W and R (samples called W_*hyg* and R_*hyg*) was performed according to the TAPPI
101 method (T 573 sp-15 2015). Glass tubes (Wheaton, 35 mm internal diameter (ID) × 147 mm, 144
102 mL) were filled with 4.0 g of paper (dry weight), i.e. 4.23 g of paper conditioned at 50% relative
103 humidity (RH) and 23 °C, based on the value of the equilibrium moisture content (EMC = 5.43
104 %_{wt}) determined with the sorption isotherm. The tubes were hermetically closed and heated at 100
105 °C in an oven (Mettler UN 55 oven) during 10 days to reach a decrease in *DP* of about 50%.
106 During *hyg* aging, the relative humidity in the tube stabilizes around 50% thanks to the moisture
107 contained in the paper so that both hydrolysis and oxidation occur. The weight-average degree of
108 polymerization (*DP_w*) of cellulose was measured using SEC-MALS-DRI (details in Physico-
109 chemical characterizations section) and the copper number (*N_{Cu}*) was determined using the
110 standard method (T 430 cm-99 1999). The total carbonyl groups concentration was derived from
111 *N_{Cu}* using the following formula proposed by Röhrling: $[CO] = \frac{(N_{Cu}-0.07)}{0.06}$ (Röhrling et al. 2002).
112 *DP_w* for W_*hyg* and R_*hyg* was 1490 ± 2% and 1961 ± 1.6%, respectively. *N_{Cu}* of W_*hyg* was 0.11.
113 Oxidative degradation (*ox*) was carried out by immersing W in an aqueous solution of sodium
114 hypochlorite (0.42-0.62% active chlorine) adjusted to pH 7 with HCl 6 N, during 15 min under
115 gentle stirring. At this pH, NaClO is known to promote enhanced carbonyl groups formation
116 (aldehyde, ketone, and carboxyl groups) on C2, C3 and C6, short chain organic acids as well as

117 considerable glycosidic scissions (Nevell 1985). The samples (called *W_ox*) were abundantly
118 rinsed with milli-Q water until neutral pH of the water, and were dried between blotters. The DP_w
119 for *W_ox* was $1352 \pm 2\%$ and N_{Cu} was 0.42.

120 Some of the *W_ox* samples additionally underwent a reduction treatment with $Na(BH)_4$ to reduce
121 the carbonyl groups produced during the aging (aldehyde and keton functions) to alcohol groups,
122 and achieve a nearly null N_{Cu} . To this end, a solution made with anhydrous $Na(BH)_4$ (Sigma)
123 (2.91g) dissolved in absolute ethanol (154 mL) was prepared, in which 1.54 g of paper was
124 immersed and left under gentle stirring during 12 hours (Burgess 1988; Carter 1996). After
125 reduction, the papers were abundantly rinsed with milli-Q water until the water reached neutral pH,
126 and were dried between blotters. The samples were called *W_red*.

127 A portion of the *W* and *R* Control samples were sized by immersing the paper sheets in a 20 g L^{-1}
128 aqueous solution of type B photographic grade gelatin from cattle bone (Gelita type restoration 1,
129 Kind & Knox) at $30 \text{ }^\circ\text{C}$ during 10 minutes. The sheets were then dried vertically at ambient
130 temperature. The sized samples were named *W_G* and *R_G*.

131 The dry gelatin uptake (UP) of *W_G* and *R_G*, determined as $UP =$
132 $\frac{m_{sized\ paper\ dry} - m_{unsized\ paper\ dry}}{m_{unsized\ paper\ dry}}$, was $4.8\% \pm 0.2$. Dry masses were calculated subtracting the EMC

133 at $23 \text{ }^\circ\text{C}$ and 50% RH measured according to the standard method (T 502 cm-07 1998). The UP
134 value falls in the range of gelatin content in historical papers (Barrow 1972; Barrett 1992) and
135 corresponds to a substantial amount of size in the paper (qualified as with '+' in Table 1).

136 Some of the *W_G* and *R_G* samples were used to apply the second compound of interest: iron
137 gallate ink, also referred to as *I* (samples called *W_GI* and *R_GI*). The ink was prepared by mixing
138 $FeSO_4 \cdot 7H_2O$ (Sigma Aldrich, 99%) (40 g L^{-1}), gallic acid monohydrate (Sigma Aldrich, 99%) (9
139 g L^{-1}) and gum Arabic (Sigma Aldrich, G9752) (140 g L^{-1}). The mixture was stirred during 3 days
140 at room temperature. The amount of gum Arabic used was purposely high in order to limit the
141 penetration of the ink inside the paper. The iron sulfate vs gallic acid ratio was adapted from a
142 recipe used in previous work (Rouchon et al. 2011). Large inked strokes (1.5 cm wide each) were
143 applied side by side with a flat-end metal pen ("Plakat", Brause) in order to cover the whole sample
144 surface. This procedure was not intended to replicate a quill pen stroke, but to provide a large and
145 homogeneous inked surface ($2 \times 1 \text{ cm}^2$). The ink penetrated 30 to 112 microns into the paper, *i.e.*
146 one third to one half of the sheet thickness, as observed with the optical microscope (Fig S1 in the

147 Supplementary data file). The iron content determined by XRF using a previously established
148 calibration curve (unpublished data) was similar in both samples: $97 (\pm 5) \mu\text{mol g}^{-1}$ in W_GI and
149 $110 (\pm 15) \mu\text{mol g}^{-1}$ in R_GI, values that are comparable to those in historical documents ($36\text{-}179$
150 $\mu\text{mol g}^{-1}$) (Rouchon et al. 2011).

151 The third compound added to the papers was CaCO_3 (samples called W_Ca). W paper was
152 immersed in a saturated aqueous solution of calcium hydroxide (95%, Sigma Aldrich) (approx. 1.4
153 gL^{-1}) during 1 hour and was dried in ambient air. This was repeated four times successively in order
154 to achieve a high calcium carbonate content. After each bath, the paper sheets were placed between
155 two blotters, and the excess solution was removed by applying a 10 kg Cobb test metal roller once
156 back and forth on the blotters. Then the sheets were dried under weight. The reaction of CO_2 with
157 the air when the paper is removed from the solution converts $\text{Ca}(\text{OH})_2$ to CaCO_3 , so-called alkaline
158 reserve (AR). The AR determined according to the standard method (T 553 om-00 2000) was 1.18
159 $\pm 0.06 \text{ mol kg}^{-1}$, otherwise expressed as equivalent $6.0\% \pm 0.3$ in CaCO_3 . Additionally, a
160 commercial permanent paper made of cotton linters, which contained 7.25% precipitated CaCO_3
161 (Krypton parchment, Spixel Inc, formerly Domtar), was used (samples named K). Because it was
162 manually prepared, Ca distribution inside W_Ca was less homogeneous than in K paper (Fig. S2
163 in supplementary data file). All the samples were conditioned prior to use at 50% RH, 23°C
164 according to the standard method (T 402 sp-08 2013).

165

166 *Archival papers*

167 Five archival paper documents from the 18th and 19th century manufactured with linen rags were
168 chosen. They were named DCN, SE, LN1, LN5, and M. They all contain gelatin size to different
169 degree, varying from light to strong, and have different *DP* (Table 1 and Fig. S3 in the
170 Supplementary data file). SE is a page from an 18th century printed volume and has a slightly
171 brownish hue, which appears darker in the center inked area of the page, due to natural aging. DCN
172 is a printed decree and has a very faint bluish hue. These two papers seem to have the lowest
173 amount of sizing (Fig. S4 in the Supplementary data file). The three other documents (LN1, LN5
174 and M) are individual folios of notarial deed documents. M is a blank paper while both LN1 and
175 LN5 are handwritten with iron gall ink. In SE, DCN, LN1 and LN5, only ink-free areas were used,
176 in order to better compare with M. Additionally, to investigate the effect of the iron gall ink on

177 ancient archival paper, the laboratory-made iron gallate ink was applied to some of the M samples
 178 using large strokes as previously described for papers W_GI and R_GI, which yielded a
 179 homogeneous inked area (sample called M_I).

180
 181 **Table 1** Samples characteristics: constituents, aging method, thickness (x), equilibrium moisture content (EMC) at 23
 182 °C and 50% RH (T 502 cm-07 1998), weight-average or viscometric-average (denoted *) degree of polymerization
 183 (DP_0), pH (T 509 om-15 2002), copper number (N_{Cu}) (T 430 cm-99 1999), concentration of total carbonyl groups
 184 ([CO]) (Röhring et al. 2002), ash content (measured at 525 °C) (T 211 om-02 2002), alkaline reserve (AR) expressed
 185 as % $CaCO_3$ (T 553 om-00 2000). Standard deviation (STD) is provided when possible. Cot: cotton papers; lin: linen
 186 rag pulp papers; ox: oxidative degradation; hyg: hygrothermal aging; red: reduction treatment; nat. natural aging; Ca:
 187 calcium carbonate filler; I: iron gallate ink; G: gelatin sizing (identified with hydroxyproline spot test, with ++: highest
 188 size content; +: medium size content; ~: lowest size content (levels defined with a water drop absorption test) (Fig S4
 189 in the Supplementary data file). n.d. stands for not determined.

190

Sample	fiber	Additive	aging	x μm	EMC % wt	DP_0	pH	$N_{Cu} / [CO]$ μmol g ⁻¹	Ash %	AR % _{eq}
W	cot	none	none	170	5.43	2948±2%	6.90±0.02	0.05	<0.1	
W_hyg	cot	none	hyg	151	5.46	1490±2%	6.2±0.2	0.11 / 0.67		
W_ox	cot	none	ox	170	n.d.	1352±2%	6.73±0.02	0.42 / 5.83		
W_red	cot	none	ox/red	170	n.d.	1431±1.1%	6.41±0.05	0.02		
W_G	cot	G+	none	170	6.13	3021±1%	5.70			
W_GI	cot	G+, I	none	170	6.90	2225*	4.21			
K	cot	Ca	none	100	5.61	2566±2%	8.89		7.6	7.3
W_Ca	cot	Ca	none	170	5.20	2803±2.2%	8.86		5.4	6.0
R	lin	none	none	160	5.78±0.18	2980	7.90			
R_hyg	lin	none	hyg	141	n.d.	1961±1.6%	6.14			
R_G	lin	G+	none	160	6.57	3326±6.8%	7.68			
R_GI	lin	G+, I	none	150	7.21	2290*	5.15			
SE	lin	G~	nat	115	5.46	1000±9.4%	5.90			
LN5	lin	G++	nat	125	5.36	1039±5.7%	4.92		1.1	
M	lin	G++	nat	125	5.75±0.04	1490±12.8%	5.03		1.5	
M_I	lin	G++, I	nat	125	n.d.	702*	n.d.			
LN1	lin	G+	nat	165	5.12	1608±2.3%	5.28		0.8	
DCN	lin	G~, Ca	nat	90	6.01	2869±6.2%	7.61		2.5	

191 Synchrotron X-ray radiation exposures

192 The papers were cut into a few cm² samples, inserted in plastic photography slide frames, and
 193 heated for 2 h at 40 °C (Memmert UN 55 oven) for gentle moisture desorption. They were then

194 placed 48 h in a climatic chamber at 23 °C and 50% RH for equilibrium moisture regain, after
195 which they were sealed in LDPE plastic bags where silica gel ProSorb (Atlantis) was added so as
196 to maintain 50% RH ($\pm 5\%$). The EMC (23 °C, 50% RH) of the papers was determined according
197 to the TAPPI test method (T 502 cm-07 1998) (Table 1). No moisture leakage was recorded upon
198 monitoring the RH inside the bags for at least 72 h prior to the synchrotron radiation (SR)
199 experiment with a temperature/humidity logger (Ibutton® Hygrochron, Measurement Systems
200 Ltd). The bags were themselves sealed with Escal® film also filled with silica gel to stabilize the
201 RH to 50% for transportation from the laboratory to the synchrotron facility.

202 The irradiation was performed on the beamline PUMA (SOLEIL synchrotron, Saclay). A
203 monochromatic beam ($2 \times 1 \text{ cm}^2$) from a double crystal monochromator (DCM) with Si(111)
204 crystals was used at photon energies of 7.22 keV, 12.5 keV or 18 keV. The samples were exposed
205 perpendicular to the beam, inside the LDPE bags. The irradiation duration varied to reach various
206 doses in the range 7 Gy to 4 kGy. The dose D (Gy) is defined as the total energy deposited per
207 mass unit of material. As it is not possible to directly measure it via dosimetric techniques, which
208 would be of limited accuracy in a heterogeneous material such as paper, it was calculated as
209 follows:

$$210 \quad D = \frac{F \cdot E \cdot t}{m} = \frac{I_0 \cdot (1 - e^{-\mu \cdot x}) \cdot E \cdot t}{\rho \cdot \sigma \cdot x}$$

211 with F , the absorbed photon flux (ph s^{-1}) ; E , the energy of X-ray photons (J) ; t , the exposure time
212 (s) ; I_0 , the incident flux (ph s^{-1}) ; m , the mass of paper (kg) ; x , the thickness of paper (cm) ; ρ its
213 density (g cm^{-3}) ; σ , the beam imprint ; μ the linear attenuation coefficient (cm^{-1}), which was
214 determined by measuring the incident and transmitted flux impinging stacked sheets as previously
215 described (Gimat et al. 2020). The dose rate was obtained by the ratio D over the exposure time.
216 For Whatman paper n°1, the dose rate was 0.71 Gy s^{-1} at 7.22 keV and 18 keV and 1.35 Gy. s^{-1}
217 at 12.5 keV.

219 **Physico-chemical characterizations**

220 After the irradiation, the samples were kept in the dark at 50% RH and 23 °C until analysis. The
221 analyses were usually performed within 6 days, the latter being the shortest possible duration

222 between the irradiation and the analysis. This allowed for immediate damage assessment. Post-
223 irradiation monitoring was carried out by regularly re-examining the samples.

224 *Molar masses*

225 The molar mass distribution and the number- and weight-average molar masses of cellulose M_n
226 and M_w were determined using Size-Exclusion Chromatography (SEC), except for the inked
227 samples which were analyzed using viscometry. For SEC, paper samples (3-5 mg) were prepared
228 and analyzed as described previously (Dupont 2003b). The precision on M_w was between 0.2 and
229 4.0 RSD%, depending on the samples.

230 S , the glycosidic scissions concentration, was calculated using DP_n , with $DP_n = \frac{M_n}{M_{AGU}} = \frac{N_{AGU}}{N_{molecule_t}}$,
231 where N_{AGU} is the total number of anhydroglucose units, i.e monomers ($M_{AGU} = 162 \text{ g mol}^{-1}$) and
232 $N_{molecule_t}$ is the total number of cellulose molecules at any time t (μmoles). As each glycosidic bond
233 scission increases by one the number of cellulose chains, the increase in the concentration of new
234 chains formed is equal to S . The number of scissions being equal to $N_{molecule_t} - N_{molecule_{t0}}$ and N_{AGU}
235 being equal to $6170 \mu\text{mol g}^{-1}$ of paper, hence $S = 6170 \left(\frac{1}{DP_{nt}} - \frac{1}{DP_{nt0}} \right) \mu\text{moles g}^{-1}_{\text{paper}}$ (Whitmore
236 and Bogaard 1994).

237 In order to avoid polluting the SEC columns with iron, DP of the gelatin-ink coated samples W_GI
238 and R_GI was measured using viscometry in cupriethylene diamine (CED) (T 230 om-19 1999)
239 with a capillary viscometer Routine 100 (Cannon-Fenske). Irradiation was carried out four days
240 after the ink application. Due to experimental constraints, the viscometry measurements were
241 carried out 29 days after the irradiation. Before the viscometry analysis, the paper samples were
242 chemically reduced with NaBH_4 (same treatment as described above) in order to avoid solvent
243 induced depolymerization. They were dried between blotters and conditioned at 50% RH and 23
244 °C. The viscometric DP (DP_v) was calculated from the intrinsic viscosity $[\eta]$ using the Mark-
245 Houwink-Sakurada equation, by applying the coefficients proposed by Evans and Wallis (Evans
246 and Wallis 1987) : $[\eta] = 0.91 \times DP_v^{0.85}$. DP_v is assumed to be very close to DP_w as M_v has been
247 reported to be closer from M_w than M_n (Ross-Murphy 1985). This allows to parallel DP_v with DP_w
248 with some confidence. The formula proposed by Dupont et al. (Dupont et al. 2018) was used for
249 the conversion of DP_v to DP_n : $DP_n = 1575 e^{(DP_w/3536)} - 1575$.

250 *Hydroxyl radicals*

251 The paper samples were soaked for 3 minutes in a methanolic solution of terephthalic acid (TPA)
252 (98%, Sigma Aldrich) (1 mM). They were left to dry at ambient temperature for 24 h and
253 conditioned at 23 °C at 50% RH. TPA reacts with hydroxyl free radicals (HO•) in the paper and
254 produces hydroxyterephthalic acid (HTPA), which accumulates in the paper. HTPA was extracted
255 from the paper (2-3 mg) by soaking during three hours in 300 µl of phosphate buffer (KH₂PO₄ 50
256 mM pH 3.2, 70% water:30% methanol), and was quantified by reverse phase liquid
257 chromatography with UV and fluorescence detection (RP-HPLC/FLD-DAD) according to a
258 previously established method (Jeong et al. 2014). HTPA (µmol g⁻¹) was calculated with respect to
259 the paper dry weight, subtracting the additives weight, to correlate sample behavior based on their
260 cellulosic content only. In order to ensure the quality of the results, it was verified that no HTPA
261 was formed upon irradiating TPA powder.

262 *Colorimetric and UV luminescence measurements*

263 The diffuse reflectance and UV luminescence of the paper samples were measured with a non-
264 invasive UV-Vis-NIR spectroradiometer (Specbos 1211UV, JETI). For UV luminescence, the
265 excitation was centered at 365 nm (with full width half-maximum FWHM = 20 nm). Measurements
266 were normalized to a blue luminescent certified reflectance standard (USFS-461 Spectralon) to
267 correct for light intensity change with time. The maximum intensity of each UV luminescence
268 spectrum was used to monitor the global intensity change. To calculate the change the following
269 formula was used:

$$270 \quad \Delta I(\lambda_{\max}) = I(\lambda_{\max})[irr] - I(\lambda_{\max})[Ctrl]$$

271 with $I(\lambda_{\max})[irr]$ and $I(\lambda_{\max})[Ctrl]$ the intensities of luminescence at the wavelength maxima
272 measured inside (irr) and outside (Ctrl) of the irradiated area, respectively.

273 A spectrophotometer (Konica Minolta, CM-26d) was used to measure the chromaticity
274 coordinates L*, a* and b* in the CIELAB 1976 system. The variation of the color coordinate b*,
275 which spans on the blue-yellow scale, was used to quantify the yellowing expressed as $\Delta b^* = b^* -$
276 b_0^* (positive value).

277

278 Results and discussion

279 Calculation of the SR X-ray dose

280 The extent of radiation damage usually depends on the X-ray dose absorbed by a sample. Different
281 papers are expected to absorb X-ray differently, especially when heavy elements are present as the
282 latter increase the absorption. Defining the X-ray dose is thus essential in order to compare changes
283 in paper samples after irradiation on a common basis. In order to do so, it is necessary to define the
284 linear attenuation coefficient (μ) of each sample for each experimental setup and condition. The
285 value of μ was measured with the incident and transmitted flux impinging stacked sheets as
286 previously described (Gimat et al. 2020). This value depends on the sample characteristics and on
287 the X-ray energy. Indeed, μ decreases with increasing energy, mainly due to the decrease of
288 photoelectric effect. The values of μ measured for W were: $4.29 \pm 0.07 \text{ cm}^{-1}$ at 7.22 keV, $1.02 \pm$
289 0.06 cm^{-1} at 12.5 keV and $0.31 \pm 0.031 \text{ cm}^{-1}$ at 18 keV. The values of μ for all the papers at 7.22
290 keV are given in Table 2. These values fell in the same range for the archival papers and the model
291 papers. As expected, the values in the table show a positive variation of μ with the paper's density
292 (ρ). Indeed, in denser papers the beam path crosses more absorbing atoms. A plot of μ vs ρ (Fig.
293 S7 in Supplementary data file) shows that for all the papers the two values are actually strongly
294 positively correlated, and that ρ explains most of the variation in μ , sometimes all the variation,
295 depending on the samples. For instance, for gelatin sized papers (W_G, R_G), degraded model
296 (W_hyg, W_ox and R_hyg) and archival papers, a higher μ compared to the Control samples was
297 ascribable exclusively to a higher paper density. However, for some samples, there was an
298 additional input to μ . This is the case for samples W_Ca and K, and was attributed to the presence
299 of Ca. Ca is a heavy element and has a higher photon absorption than the atoms in cellulose. It was
300 thus expected that Fe in the inked samples would have the same impact on μ when compared to the
301 counterpart samples with no ink. This was indeed the case for R_GI and M_I, but not for W_GI
302 (Fig. S7 in Supplementary data file).

303

304 **Table 2** Linear attenuation coefficient μ (cm^{-1}) with standard deviation and density (ρ) of the studied papers at 7.22
305 keV, 50% RH.

306

	Cotton papers		Linen rag papers		Archival papers (gelatin sized)			
	μ cm ⁻¹	ρ g cm ⁻³	μ cm ⁻¹	ρ g cm ⁻³	μ cm ⁻¹	ρ g cm ⁻³		
W	4.29 ± 0.07	0.51	R	5.01 ± 0.25	0.54	LN5	5.60 ± 0.23	0.62
W_G	4.76 ± 0.02	0.54	R_G	4.77 ± 0.07	0.53	M	5.69 ± 0.03	0.47
W_GI	7.03 ± 0.04	0.62	R_GI	7.99 ± 0.08	0.55	M_I	10.05 ± 0.03	0.72
W_Ca	6.89 ± 0.12	0.54				SE	6.66 ± 0.04	0.64
K	9.56 ± 0.20	0.68				LN1	7.21 ± 0.10	0.68
W_hyg	5.32 ± 0.07	0.55	R_hyg	5.69 ± 0.28	0.60	DCN	8.18 ± 0.60	0.72
W_ox	5.66 ± 0.14	0.53						
W_red	5.28 ± 0.04	0.53						

307

308 *DP and hydroxyl radicals*

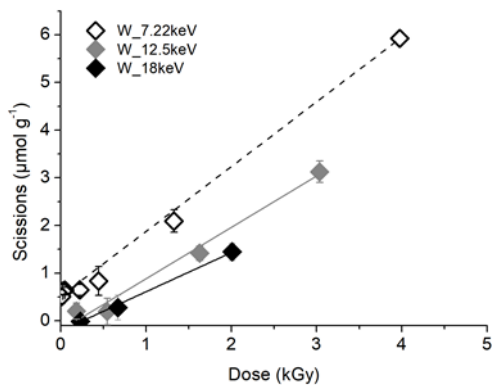
309 Impact of the X-ray dose and photon energy

310 All the X-ray radiation exposures were carried out on the PUMA beamline at synchrotron SOLEIL.
311 Nevertheless, a first experiment, was carried out with a laboratory Micro X-ray Fluorescence
312 Spectrometer (methodology in the Supplementary data file), to allow assessing the impact of low
313 doses in the range of those usually delivered by these laboratory instruments. All the unaged W
314 samples, irradiated to a dose up to 22 Gy, had a similar *DP* to the Control sample (Fig. S8 in the
315 Supplementary data file), indicating that no macromolecular degradation took place during the
316 irradiation, whether the dose was delivered at once or in several stages. This is consistent with the
317 lowest observable adverse effect dose (LOAED) for glycosidic scissions of 0.21 kGy defined in
318 our previous work (Gimat et al. 2020).

319 Synchrotron X-ray fluorescence experiments usually use energies in the range of 1 to 20 keV
320 (Glaser and Deckers 2014), sometimes even higher if heavy elements are investigated. To
321 investigate if the degradation was energy dependent, W samples were exposed to three photon
322 energies: 7.22, 12.5 and 18 keV. Fig. 1 shows the glycosidic scissions concentration (*S*) as a
323 function of the absorbed dose up to 3.9 kGy, at the three energy levels. *S* increased with the dose
324 in the range of 0 to 6 $\mu\text{mol g}^{-1}$. The impact was very small below the LOAED (0.21 kGy) and was
325 followed by a linear increase from 0.5 kGy upwards. *S* increased steeply, similarly at 12.5 keV and
326 18 keV. At 7.22 keV, all the values of *S* were shifted up. A similar energy dependence has been
327 observed for electron beam irradiation (Bouchard et al. 2006) at energies of several MeV. While

328 the photoelectrons created by the X-ray photons in our experiment have much lower energies, it
329 seems like the inverse relation between kinetic energy and cellulose damage remains true in the
330 keV regime. We are not sure why this is the case, but it is noteworthy that the inelastic mean free
331 path (IMFP) varies considerably for electron energies in the range of our experiment compared to
332 the typical average diameter of cellulose fibers. The IMFP for electrons in graphite changes from
333 9.2 nm at 7.3 keV to 19.5 nm at 18 keV (Shinotsuka et al. 2015). While the exact path lengths in
334 cellulose will likely be slightly different, this shows that it is thus much more probable that a
335 photoelectron produced by 18 keV X-rays escapes the cellulose fibers before causing damage than
336 it is for one produced by 7.22 keV X-rays. Although a lower dose rate can sometime increase
337 material damage (Adamo et al. 2001), this was not observed here since glycosidic scissions
338 concentration was higher at 7.22 keV than at 18 keV at similar dose rate (0.7 Gy^{-1}), yet it was
339 intermediate at 12.5 keV at higher dose rate ($1.35 \text{ Gy} \cdot \text{s}^{-1}$) (Fig. 1). Based on these results, all the
340 following experiments were carried out at 7.22 keV, the most penalizing conditions, to enhance the
341 chances of observing and characterizing damage.

342



343

344 **Fig. 1** Glycosidic scissions concentration S as a function of the X-ray dose in Whatman n°1 irradiated at energy of
345 7.22, 12.5 and 18 keV at 50% RH

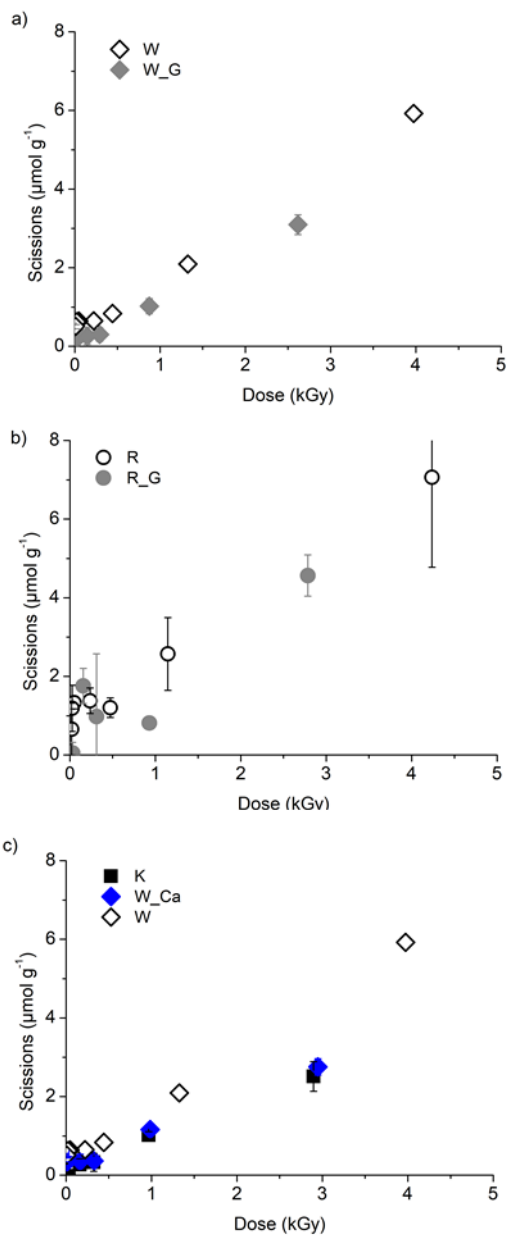
346 Impact of calcium carbonate and gelatin

347 The glycosidic scissions and hydroxyl free radicals concentrations in the unaged papers, in the
348 papers with calcium carbonate and in the papers with gelatin increased in a quasi linear fashion as
349 a function of the X-ray dose, up to $6 \mu\text{mol g}^{-1}$ for W and up to $8 \mu\text{mol g}^{-1}$ for R (Figs. 2 & 3). S in
350 W_G was slightly lower than in W Control (Fig. 2a). This is consistent with the fact that gelatin

351 size tends to lower the depolymerization rate of cellulose during the degradation induced by aging
352 (Dupont 2003a). Besides gelatin, this could also be partly due to the difference in moisture in
353 unsized vs sized paper (EMC at 23°C of 5.43% and 6.13%, respectively), as moisture was shown
354 to reduce cellulose depolymerization during synchrotron X-ray irradiation (Gimat et al. 2020).
355 Because of a larger standard deviation on the data points, this was less clearly established for R
356 and R_G, where *S* values were quasi similar (Fig. 2b) despite the EMC difference (5.78% vs 6.57%,
357 respectively) (Table 1).

358 The samples with gelatin (W_G and R_G) produced less hydroxyl radicals than the Control
359 samples (Fig. 3a and 3b). This could be an indication that gelatin was able to scavenge the HO•
360 produced during the irradiation.

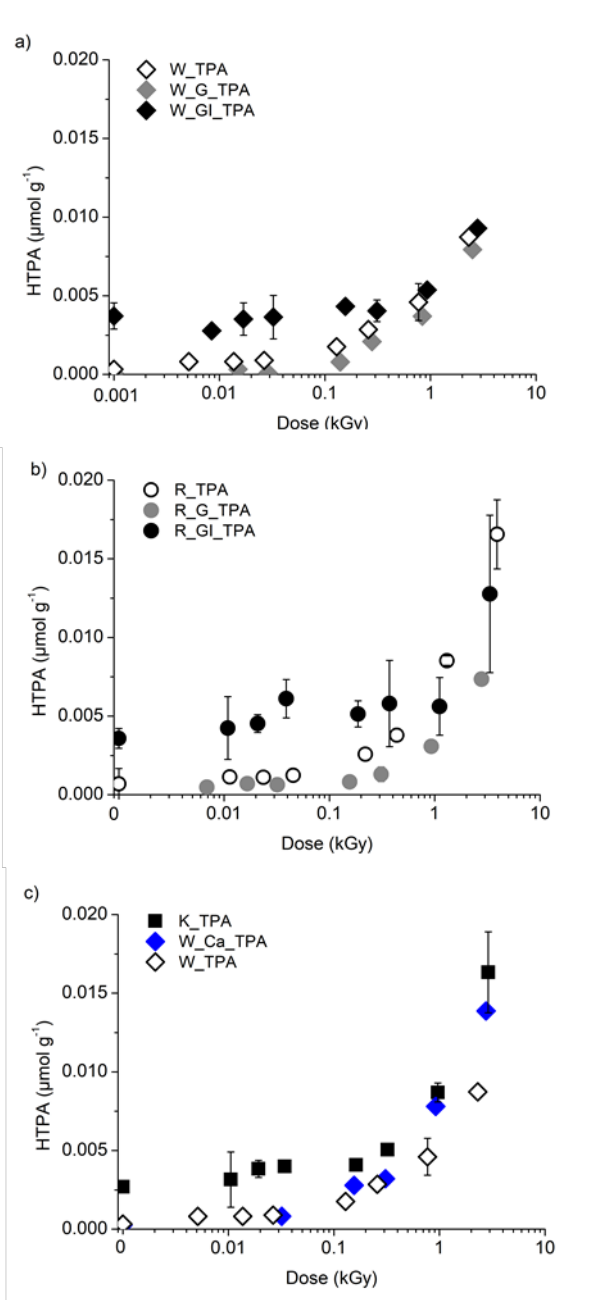
361 In both W_Ca and K, *S* increased slightly less as a function of the dose than in W Control, which
362 is especially visible at the high doses, as shown on Fig. 2c. this suggests that calcium carbonate
363 can buffer the organic acids generated by cellulose degradation caused by the X-ray exposure,
364 which is the expected role of the alkaline reserve in paper (Whitmore and Bogaard 1994; Ahn et
365 al. 2013; Rouchon and Belhadj 2016). On the other hand, W_Ca and K showed a larger HO•
366 production than the Control samples (Fig. 3c). This, again, could be due to the pH, as an alkaline
367 medium is known to enhance the lifetime of HO• radicals, and hence the probability that they react
368 with TPA. These results also confirmed previous observations that the HO• concentration did not
369 always correlate directly with the glycosidic scissions concentration, and indicate that other species
370 and mechanisms are involved (Jeong et al. 2014; Gimat et al. 2020).



372

373 **Fig. 2** Glycosidic scissions concentration (S) in W and R Control papers, papers with gelatin (W_G and R_G) (a, b)

374 and with calcium carbonate (W_Ca and K) (c), as a function of X-ray dose after irradiation at 7.22 keV.



375

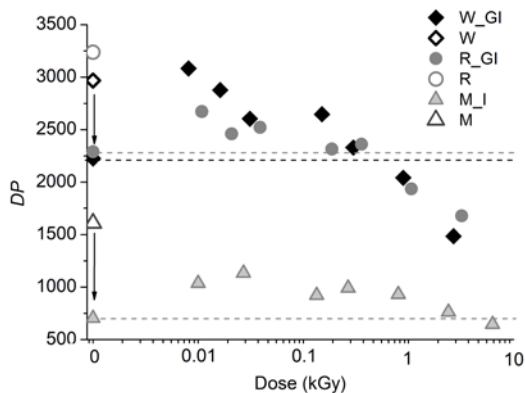
376 **Fig. 3** Impact of gelatin, iron gallate ink (a, b) and calcium carbonate (c) in W and R papers on the HTPA
 377 concentration as a function of X-ray dose after irradiation at 7.22 keV. The logarithmic scale is used for easier
 378 visualization.

379

380 Impact of the iron gallate ink

381 For the three samples coated with the iron gallate ink (W_GI, R_GI and M_I), the *DP* of the non-
 382 irradiated samples was considerably lower than that of the Control samples (W, R and M) is

383 represented by the arrows on Fig. 4. This was attributed to strong and almost instant acid hydrolysis
384 and oxidation reactions due to the presence of iron gallate ink, which occurs within the period
385 between sample preparation and analysis (33 days). This has been observed previously (Rouchon
386 et al. 2011, 2016). Indeed, a *DP* loss of 25% and 30% was measured for W_GI and R_GI,
387 respectively, which is consistent with previous observations (Rouchon et al. 2011) for inked
388 Whatman n° 1 where a 24% *DP* loss was recorded within a similar timeframe. For M_I samples,
389 the *DP* loss was 50%. A striking observation was made in the low doses range: after irradiation (up
390 to 0.29 kGy for W_GI, 0.36 kGy for R_GI and 2.4 kGy M_I), the *DP* of the iron gallate ink coated
391 samples was higher than the *DP* of their non-irradiated counterpart (Fig. 4, dashed lines). This is
392 the reason why *DP* is represented instead of glycosidic scissions as y-axis on Fig. 4. This was
393 interpreted as having two possible causes. First, it has been shown that iron gallate ink containing
394 papers produce free radicals, such as HO• and other reactive oxygen species (Gimat et al. 2016,
395 2017). This enhances the chances for free radicals recombination leading to the auto-oxidation
396 termination reactions, and in turn would lower the concentration of radicals accumulated in the
397 paper, thus, possibly preserving cellulose from their attack. Conversely in the Control samples,
398 unexposed to X-rays, the free radicals would induce a higher level of degradation. Secondly, the
399 crosslinking induced by the recombination of cellulosic radicals could lead to an increase in *DP*
400 which would be measurable if the radicals have a relatively high molar mass. This is consistent
401 with the fact that in the low irradiation doses range, HTPA was produced in higher amount in the
402 irradiated ink coated samples W_GI and R_GI than in the Control counterparts W and R (Fig. 3a,
403 3b), and in similar amount as in non-irradiated W_GI and R_GI. In the higher doses range (from
404 0.89 kGy for W_GI, 1.1 kGy for R_GI, and 6.3 kGy for M_I), the samples reached a lower *DP*
405 than the non-irradiated samples, and the HTPA concentration in the samples reached similar levels
406 with and without ink. This was interpreted as an indication that the enhanced scissions induced by
407 the irradiation at the high doses likely exceeded the supposed impact of the free radicals
408 recombination reactions.
409



410

411 **Fig. 4** Viscometric-average degree of polymerization (DP_v) of iron gallate ink coated papers W_GI (a), R_GI (b),
 412 and M_I (c) as a function of X-ray dose (kGy) after irradiation at 7.22 keV. The dose is represented on a logarithmic
 413 scale for easier visualization. Control samples without ink or gelatin are represented by the void data points. Arrows
 414 represent the DP drop due to the iron gallate ink. At low X-ray doses, irradiated samples have a higher DP than non-
 415 irradiated Control sample (above the dotted lines)

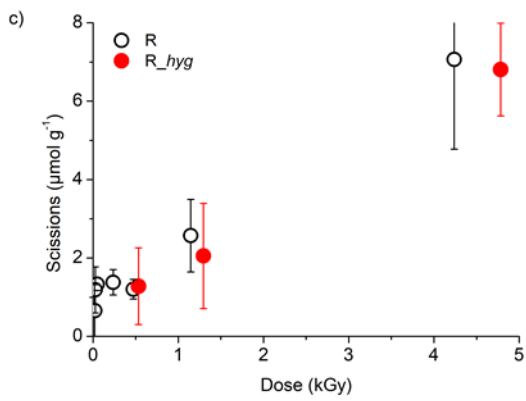
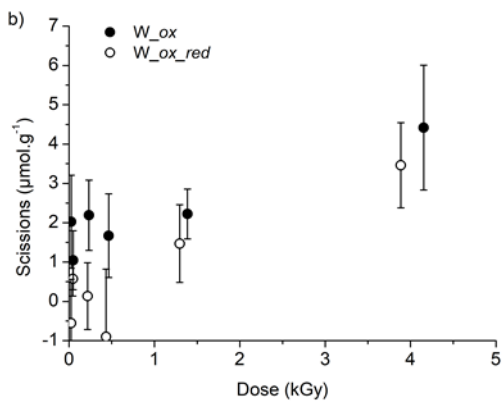
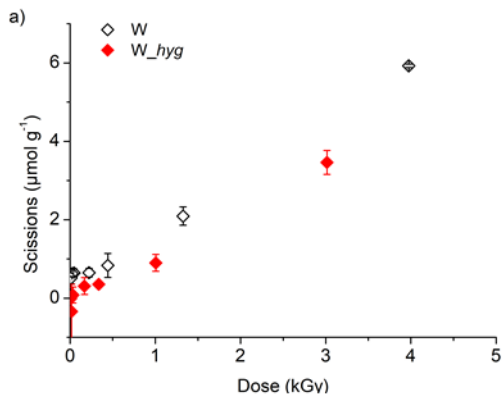
416

417 Impact of the degradation state

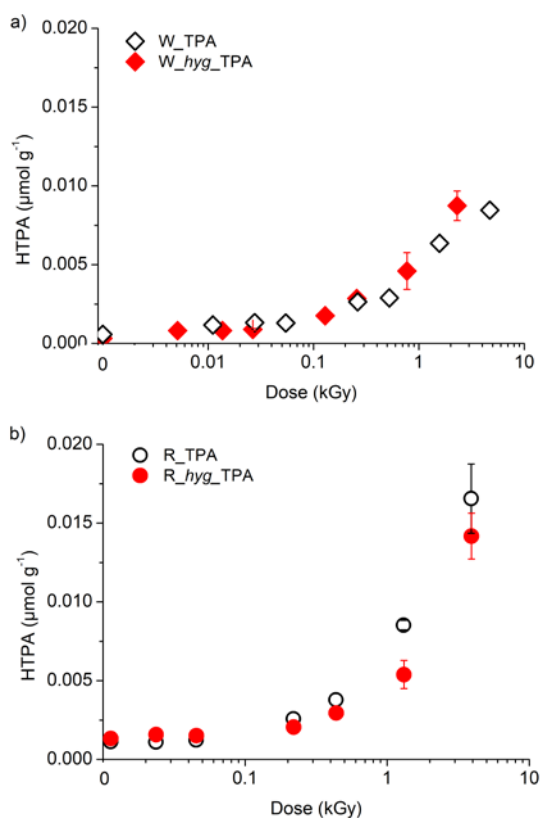
418

419 The artificially degraded papers (W_{hyg} , W_{ox} and W_{red}) were irradiated at 7.22 keV to
 420 various doses to study if and how the degradation state modifies the impact of the X-rays exposure.
 421 The intent was to possibly extrapolate the results to centuries-old cultural heritage paper. The three
 422 samples had a similar starting DP ($DP_w \approx 1400$, *i.e.* about 50% lower than W) and a different
 423 oxidation state: $N_{Cu} = 0.42$ for W_{ox} (*i.e.* $5.83 \mu\text{mol g}^{-1}$ total carbonyl groups, as calculated
 424 according to (Röhrling et al. 2002), $N_{Cu} = 0.11$ for W_{hyg} (*i.e.* $0.67 \mu\text{mol g}^{-1}$ total carbonyl groups)
 425 and $N_{Cu} = 0.02$ for W_{red} (*i.e.* near-zero carbonyl groups besides the reducing ends) (Table 1).
 426 Figures 5a and 5b show the glycosidic scissions concentration in these samples as a function of the
 427 dose. In W_{hyg} , S increased linearly with the dose, yet slightly less than in W Control (Fig. 5a).
 428 This suggests that lower DP and/or higher carbonyl groups concentration might lessen somewhat
 429 the impact of X-rays (Fig S7 in the Supplementary data file). For samples that underwent oxidation
 430 (W_{ox} and W_{red}), S was in the same range (up to $6 \mu\text{mol g}^{-1}$) as for W and W_{hyg} at respective
 431 doses (Fig. 5b), yet with higher standard deviations. The main contrast between the two samples is
 432 in the low dose region. In the range –up to 0.5 kGy, while W_{red} underwent fewer glycosidic
 433 scissions, in W_{ox} S was higher than in the other samples, with a sharp increase to 1-2 $\mu\text{mol g}^{-1}$ for
 434 doses below 1.4 kGy. This tends to indicate that at low doses, a high concentration of carbonyl

435 groups in the paper may enhance the X-ray induced depolymerization. In the higher doses range
436 (≥ 1 kGy), the depolymerization of all the samples reached the same range, between 4 and 6 μmol
437 g^{-1} . Fig 6a shows that a similar amount of HO^\bullet free radicals was produced in *W_hyg* and in *W*,
438 indicating that the free radicals were not fully responsible for the difference in the glycosidic
439 scissions, and that the HO^\bullet were not significantly involved in the production of carbonyl groups.
440 The results for the linen rag model papers are more difficult to interpret. *S* extended higher (up to
441 $8 \mu\text{mol g}^{-1}$) and increased linearly as a function of the dose, yet, in a similar way for the undegraded
442 Control sample and for the degraded *R_hyg*, despite the *DP* of the latter being 34% lower ($DP_w \approx$
443 *1961*) (Fig. 5c). Moreover, above 0.1 kGy, slightly less HO^\bullet free radicals were detected in *R_hyg*
444 than in *R* (Fig. 6b). This, and the large standard deviations on each data point of *R* samples muddles
445 the interpretations. The extrapolation of the results from a simple machine-made cellulosic paper
446 to a traditional handmade rag pulp paper is not straightforward. The next level of complexity, which
447 was to test the response of archival papers, was thus anticipated as very challenging.



448
 449 **Fig. 5** Glycosidic scissions concentration (S) in aged papers W (a, b) and aged rag papers R (c) as a function of X-ray
 450 dose compared to respective Control samples.



451 **Fig. 6** HTPA concentration in Control samples, aged W (a) and aged R (b) as a function of X-ray dose.

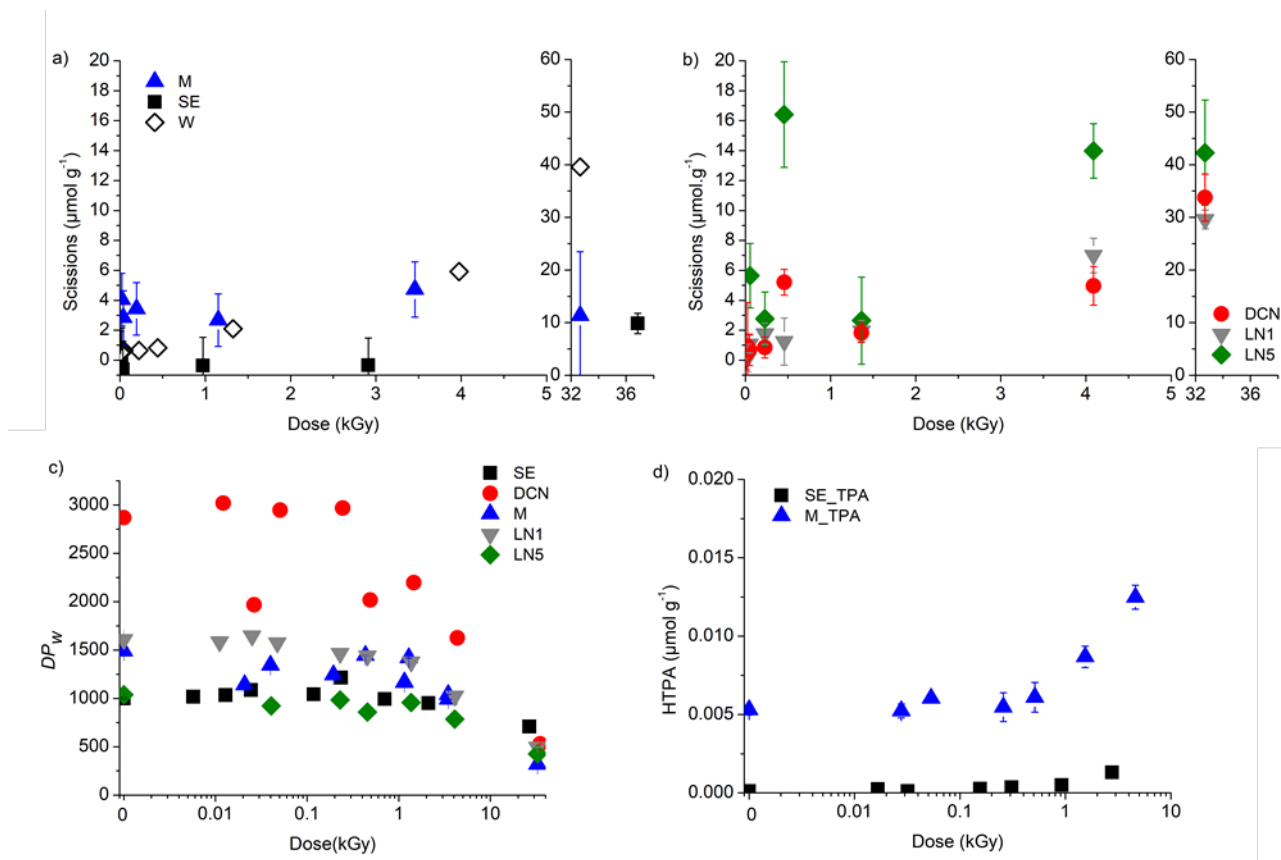
452

453 **Archival paper documents**

454 For the historic samples irradiated to various doses, *S* values were overall in the same range as
 455 those measured for the model samples. Only LN5 degraded more and showed *S* values at least
 456 twice as high as for the other archival papers at all the doses tested (Figs. 7a, 7b). However, the
 457 depolymerization behavior with increasing dose was not progressive as observed for the model
 458 papers (except for LN1), especially in the low doses. For instance, SE did not undergo scissions
 459 below 3 kGy, and M had a constant degradation (plateau) response on the whole dose range, with
 460 *S* around 3.5 μmol g⁻¹ (Fig. 7a). No correlation could be made with the *DP* (table 1), or the paper
 461 constituents. All the papers have similar iron and calcium content, except maybe DCN which has
 462 more calcium due to the calcium carbonate filler and slightly more Fe (Fig. S6 in the Supplementary
 463 data file). The other possible difference in composition would be the gelatin content, the latter
 464 being a factor that tends to lower the degradation in the model papers. Unfortunately, the gelatin
 465 content of the archival papers was unknown and could not be measured. However, an indirect

466 indication of sizing was given by a water drop absorption test, which showed that M and LN5 were
467 more hydrophobic than DCN (fig. S4 in the Supplementary data file). Even though there can be
468 other reasons for paper hydrophobicity such as reduced porosity for instance, the former two
469 showed higher S than the latter, which would tend to invalidate the aforementioned protective role
470 of gelatin. The differences in S could thus arise from local heterogeneity and to samples' structural
471 parameters such as porosity or constituents' composition. This was not unexpected as in handmade
472 papers the additives are usually not as homogeneously distributed at the microscopic level as in
473 industrial papers.

474 Very high doses, between 32 and 38 kGy, were then tested on the archival papers, as well as on W.
475 The results showed that DCN, LN1 and LN5 were similarly extensively degraded as W, with S
476 comprised between 30 and 43 $\mu\text{mol g}^{-1}$ (Figs 7a & 7b). M and SE resisted surprisingly well, being
477 the least degraded samples, with S close to 10 $\mu\text{mol g}^{-1}$. Despite the different kinetics, most samples
478 approached LODP (Levelling Off Degree of Polymerization) with DP_w W = 345; DP_w M = 318;
479 DP_w LN5 = 426; DP_w LN1 = 495. The least degraded samples were DCN (DP_w = 530) and SE (DP_w
480 = 708) (Fig. 7c). The production of HO^\bullet free radicals was measured in SE and M. In SE, HO^\bullet
481 concentration was very low, but it was higher in M over the whole dose range reaching a similar
482 amount as in the model papers containing Ca and Fe (Fig. 7d). This difference was thus attributed
483 to the slightly higher calcium and iron content in M than in SE (Fig. S6 in the Supplementary data
484 file).



486

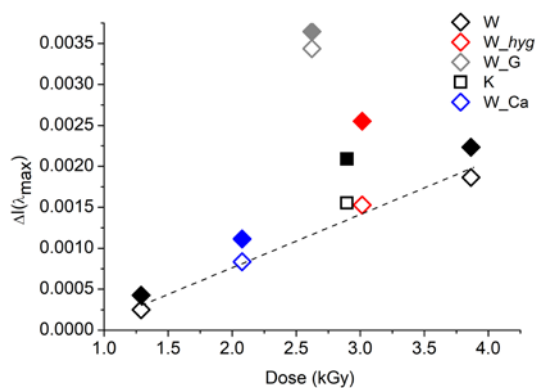
487 **Fig. 7** Glycosidic scissions concentration (S) (a, b), DP_w (c) and HTPA concentration (d) in archival samples as a
 488 function of X-ray dose. Logarithmic scale (c-d) is used only for a better display of the data.

489

490 *UV Luminescence and yellowing*

491 Before the irradiation, all the samples, model and archival, exhibited luminescence under UV when
 492 excited at 365 nm, which is a common feature of paper (Fig. S9 in the Supplementary data file).
 493 The model samples W and R exhibited a luminescence maximum λ_{max} at 432 nm, which is
 494 consistent with previous data (Gimat et al. 2020). The intensity varied depending on the type of
 495 additive and on the degradation state, luminophores being produced during the aging. For instance
 496 gelatin is expected to show a broad luminescence spectrum with $\lambda_{\text{max}} = 402$ nm (unaged) and 414
 497 nm (artificially aged at 50% RH and 80° C) (Yova et al. 2001; Duconseille et al. 2016). After X-
 498 ray exposure, no change in the UV luminescence spectral distribution was observed during the
 499 three years monitoring period. The intensity at λ_{max} [$I(\lambda_{\text{max}})$] of each spectrum was followed over

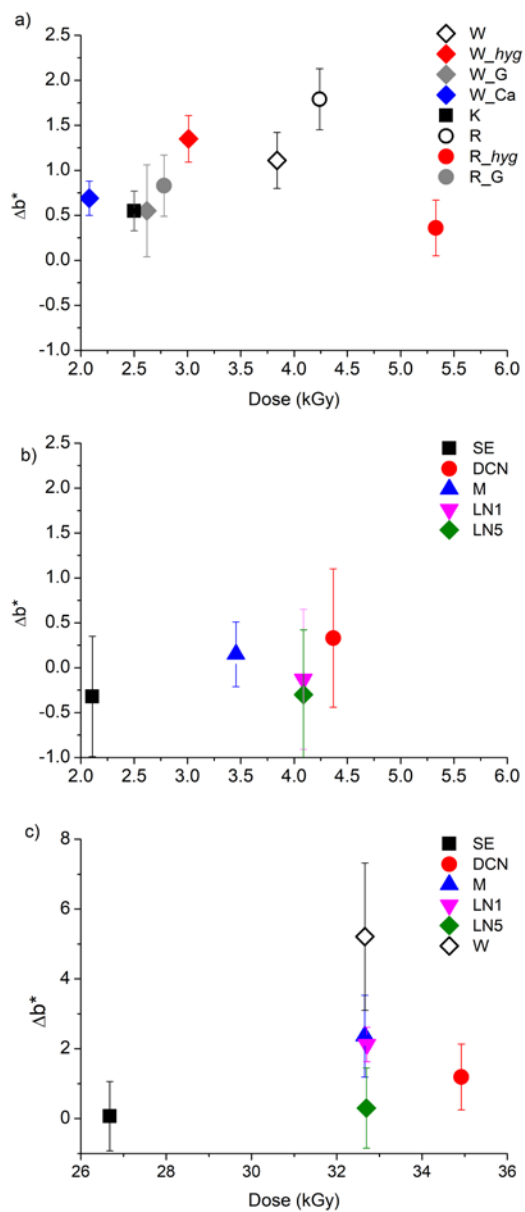
500 time. After eight months, the area of the model papers irradiated at 7.22 keV (dose range from 2.8
 501 to 4 kGy, depending on the sample) exhibited an increase in the intensity of the UV luminescence
 502 compared to the respective Control samples ($\Delta I(\lambda_{\max})$), as shown Fig. 8 and Fig. S10
 503 (Supplementary data file). All Whatman n° 1 model papers (except for the sized samples), showed
 504 luminescence proportionally to the absorbed dose (Fig 8, white marks, linear trendline). The
 505 highest increase in luminescence was observed on the sized samples W_G and R_G with
 506 $\Delta I(\lambda_{\max})_{R_G}$ of 0.0042 and $\Delta I(\lambda_{\max})_{W_G}$ of 0.0036 (R_G data not shown), indicating that a large
 507 quantity of luminophores was produced post-irradiation. These samples were still the most
 508 luminescent samples after 11 months. The luminescence of W_hyg and K grew beyond that of the
 509 other samples between 8 and 11 months. The change in luminescence between unaged and aged R
 510 papers (with no additives) was slower than for unaged and aged W, with a smaller $\Delta I(\lambda_{\max})$ of R
 511 and R_hyg (0.0011 and 0.00015, respectively) compared to W and W_hyg ($\Delta I(\lambda_{\max})$ (0.0022 and
 512 0.0025, respectively).



513
 514 **Fig. 8** $\Delta I(\lambda_{\max})$ of W, 8 months (empty marks) and 11 months (full marks) after X-ray irradiation. $\Delta I(\lambda_{\max})$ is the
 515 subtraction of the luminescence of the non-irradiated area from that of the irradiated area. The trendline represents the
 516 dose/luminescence response in W Ctrl samples.

517
 518 Colorimetric measurements were carried out three years after the irradiation, on the irradiated areas
 519 and the non-irradiated Control samples (Fig. 9). All the model samples showed very small Δb^*
 520 values (Fig. 10a) and a global color change ΔE^* between 0.55 (for K) and 1.87 (for R), *i.e.* below
 521 the usually accepted level for a just noticeable difference. Among the W samples, the artificially
 522 aged W_hyg had the highest Δb^* (1.35 ± 0.26). The opposite trend was observed with R samples,
 523 where R_hyg had a lower Δb^* than R. This observed behavior difference is all the more valid since

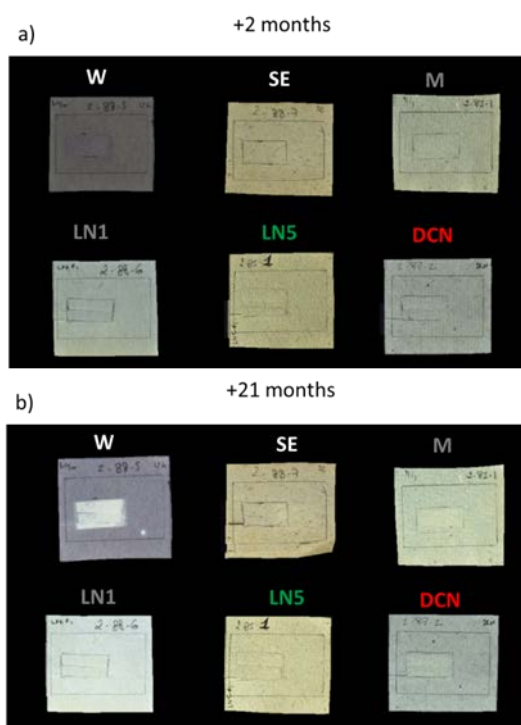
524 the data points for R on Fig 10a correspond to higher doses than for W samples and that R_{hyg} is
525 the most strongly irradiated sample. This may indicate complex radiochemistry mechanisms of
526 chromophore destruction and chromogens formation. As opposed to the observations after
527 hygrothermal aging of gelatin sized papers (Dupont 2003a; Missori et al. 2006), the irradiation did
528 not modify the yellowing in the gelatin sized papers. This may be related to the radical scavenging
529 properties of gelatin, which could lower the kinetics of cellulose chromophores formation. To sum
530 up, for the model samples, gelatin was the additive that had the highest impact on luminescence.
531 This is most probably due to its own intrinsic luminescence properties and maybe also to its
532 chromogenic degradation products appearing post-irradiation. Yellowing did not appear to be
533 linked to either the initial degradation state nor to the presence of additives, which indicates
534 complex mechanisms at play of chromogenic structure formation and destruction.
535



536
 537 **Fig. 9** Yellowing increase (Δb^*) of papers measured three years after X-ray irradiation at 7.22 keV on W and R
 538 model papers (a) and on the archival papers (b, c).
 539

540 The initial UV luminescence spectra of the archival papers showed maxima with different
 541 intensities $I(\lambda_{\max})$ and positions (between 444 nm and 460 nm), which could be due to differences
 542 in the quantity and the type of UV-absorbing groups such as carbonyl compounds, respectively.
 543 This could also be due to a different moisture content, as the latter has been shown to affect the
 544 luminescence properties of paper (Kocar et al. 2005; Castellán et al. 2007). Before irradiation, no

545 correlation between the state of degradation (*DP*) and the intensity of the luminescence of the
546 papers could be made. Indeed, LN1 and M, both with similar *DP* around 1500, displayed more
547 intense luminescence than the other historic samples, either more degraded (DP_w LN5 = $1039 \pm$
548 5.7% , and DP SE = $1000 \pm 9.4\%$) or less degraded (DP DCN = $2869 \pm 6.2\%$). The presence of
549 gelatin could not be fully responsible of the luminescence intensity either, as the the hydrophobic
550 properties - used as an indication of the gelatin content - did not correlate with luminescence (M
551 and LN5 highly hydrophobic, LN1 medium hydrophobic, SE and DCN not hydrophobic).
552 After irradiation at doses below 4.4 kGy no change was observed on the archival papers. Indeed,
553 no differences in the UV luminescence (data not shown) nor the yellowing ($\Delta b^* < 1$) were
554 measured in the irradiated vs the non-irradiated areas (Fig. 9b). At the highest doses tested (26-36
555 kGy), a slight luminescence appeared on M and DCN twenty-one months after the irradiation (Fig.
556 10). It thus took almost two years for the luminophores to build up inside the archival papers.
557 Similarly, as with the model samples, no correlation between the luminescence and the *DP*, or the
558 glycosidic scissions could be made. A test was made by irradiating M at a very high dose (290
559 kGy), which induced marginal luminescence, and only after ten months (data not shown).



560
561 **Fig. 10** Photographs under UV light of W and archival papers exposed to X-ray radiation at doses between 26 and 33
562 kGy, 1 month (a) and 21 months (b) after the irradiation at 7.22 keV.
563

564 Within the high dose range (26-36 kGy), no change was observed for SE and LN5, and the other
565 archival samples (DCN, M, LN1) exhibited a slight yellowing, with Δb^* of 1.2, 2.4, and 2.1,
566 respectively (Fig. 9c). The strongest yellowing was recorded on W ($\Delta b^* = 5.2 \pm 2.1$).

567

568 **Conclusion**

569 Synchrotron X-ray radiation at energies and doses most often applied for analytical purposes to
570 paper-based cultural heritage has been shown to be detrimental to one-component cellulosic paper
571 (Whatman n°1). However, field situations are complex as historic papers are multiparametric,
572 which interferes with a prediction of the effect of X-ray radiation. They usually are degraded to
573 some extent and they contain other constituents besides biopolymers, such as papermaking
574 additives, ink and their degradation by-products. The present research investigated how these
575 parameters, when studied individually in model papers, could influence the X-ray radiation-
576 induced degradation. The papers were artificially aged and/or supplemented with additives, which
577 enabled to single out some of the influential parameters. The additives tested were gelatin as sizing
578 agent, and calcium carbonate as filler. Iron gallate ink was applied on some of the gelatin-sized
579 papers, modeling writing/drawing medium. Following the same methodological approach as
580 developed in a previous publication (Gimat et al 2020), the changes were measured immediately
581 after the irradiation at the microscopic level (macromolecular and molecular degradation) and the
582 macroscopic changes embodied by the optical properties (UV luminescence and yellowing) were
583 monitored time-delayed.

584 In the dose range up to 4 kGy, gelatin-sized samples and samples with CaCO_3 underwent a slightly
585 reduced irradiation-induced depolymerization. Surprisingly, up to 0.89-1.1 kGy, the iron gallate
586 ink coated papers had a higher DP than the Control samples, which was attributed to a decrease in
587 the impact of the free radical initiated autooxidation reactions through radicals recombination and
588 crosslinking. Above these doses, a higher rate of scissions induced by the irradiation prevailed. The
589 production of hydroxyl free radicals was higher in all the samples containing CaCO_3 , maybe due
590 to the increased lifetime of HO^\bullet at alkaline pH. The depolymerization behavior of the aged model
591 samples was different in the industrially-made (Whatman n° 1) and in the handmade papers (linen
592 rags). Higher degradation state (lower DP) tended to stabilize Whatman n°1 paper towards X-ray
593 radiation, by lowering the macromolecular degradation. Conversely, the aged handmade paper

594 showed a similar amount of glycosidic scissions as the unaged counterpart. Carbonyl groups in the
595 artificially aged Whatman n°1 papers seemed to increase the glycosidic scissions in the low doses
596 range, below 0.5 kGy. Confirming previous results (Gimat et al. 2020), the optical changes
597 appeared with considerable delay, often one year after the irradiation, and could not be directly
598 correlated to the initial *DP* nor to the glycosidic scissions concentration that grew steadily during
599 this post-irradiation period (dark storage, room temperature). As expected, the archival papers
600 made of linen rags had an overall more complex X-ray exposure behavior than the model papers.
601 Their behavior under X-ray was multifactorial and difficult to predict, whether in terms of *DP*
602 losses (the largest being for DCN and LN1), luminescence (M and DCN exhibited the higher
603 luminescence intensity), or yellowing (M and LN1 yellowed the most). These observations led to
604 the conclusion that in the samples with additives and in the aged/degraded samples, optical changes
605 (yellowing and luminescence) were mostly uncorrelated. Moreover, as observed with the model
606 papers, these optical changes were also not directly correlated with the macromolecular state
607 (depolymerization). These observations underline the complex chemistry triggered by the exposure
608 to X-rays. At very high doses (26-36 kGy), the archival papers reached the LODP immediately
609 upon irradiation, similarly as Whatman n° 1. No color change or UV luminescence were observed
610 within one year after the exposure at those high doses. Twenty-one months after the irradiation,
611 two archival papers showed a slight UV luminescence. These contrasted results indicate that
612 laboratory samples have their limitations to model archival/historic papers and that the
613 radiochemistry at play is complex. However, the observation that, overall, the historic papers
614 resisted better the X-ray exposures than modern papers is an important step forward that enables
615 to consider analyzing historic papers with better confidence. This work focused on the paper
616 material in chemical terms. Considering paper microstructure properties in the future may shed
617 more light on the limitations encountered.

618 The results of this work underline the significance of studying the damage to artworks induced by
619 X-ray technical examination. A significant outcome was to show the importance of carefully
620 choosing the analytical conditions that limit the exposure, thus the dose, when analyzing genuine
621 artefacts using X-rays. This can be achieved either by applying higher energy, or using low
622 exposure times, and always maintaining some humidity in the paper, as demonstrated in our
623 previous work. The mid-range relative humidity value recommended for paper-based cultural
624 heritage storage is thus a good compromise. Documenting the exact location of the X-ray photons

625 impact and implementing a long-term monitoring of the eventual changes through regular
626 photographic follow-up under both UV and visible lights are advisable.
627

628 **Acknowledgements**

629 We are grateful to synchrotron Soleil for the access to the PUMA beamline within the proposal
630 20181723 and to Tülin Okbinoglu for technical help on the beamline. We thank Samia Rebaa and
631 Naomi Nganzami Ebale, undergraduate chemistry students (Sorbonne Université), for help with
632 photography and spectroscopy. We also thank Sabrina Paris Lacombe and Oulfa Belhadj for
633 technical help with Size Exclusion Chromatography and Scanning Electron Microscopy,
634 respectively.
635

636 **Funding**

637 This research was supported by Paris Seine Graduate School of Humanities, Creation, Heritage,
638 Investissements d’Avenir ANR-17-EURE-0021-Foundation for Cultural Heritage Science.

639 **Authors contributions**

640 Methodology: AG, ALD, MT, SC; PUMA Irradiation Experiment: AG, SC; physico-chemical
641 characterizations: AG, Writing-original draft preparation: AG, ALD; Writing-review and editing:
642 AG, ALD, MT, SC; Supervision: ALD, MT, SC.

643 **Conflict of Interest**

644 The authors declare that they have no conflict of interest.

645 **References**

- 646 Adamo M, Brizzi M, Magaudda G, et al (2001) Gamma radiation treatment of paper in different
647 environmental conditions: chemical, physical and microbiological analysis. *Restaurator*
648 22:107–131
- 649 Ahn K, Banik G, Potthast A (2012) Sustainability of Mass-Deacidification. Part II: Evaluation of
650 Alkaline Reserve. *Restaurator* 33:48–75. <https://doi.org/10.1515/res-2012-0003>
- 651 Ahn K, Rosenau T, Potthast A (2013) The influence of alkaline reserve on the aging behavior of
652 book papers. *Cellulose* 20:1989–2001. <https://doi.org/10.1007/s10570-013-9978-3>
- 653 Albertin F, Astolfo A, Stampanoni M, et al (2015) Ancient administrative handwritten
654 documents: X-ray analysis and imaging. *J Synchrotron Radiat* 22:446–451.
655 <https://doi.org/10.1107/S1600577515000314>

- 656 Barrett T (1992) Evaluating the effect of gelatin sizing with regard to the permanence of paper.
657 In: The Institute of Paper Conservation: conference papers Manchester 1992. Institute of
658 paper conservation, Manchester, pp 228–233
- 659 Barrow WJ (1972) Manuscripts and Documents: Their Deterioration and Restoration, 2nd
660 edition. University Press of Virginia
- 661 Bertrand L, Schöeder S, Anglos D, et al (2015) Mitigation strategies for radiation damage in the
662 analysis of ancient materials. *TrAC Trends Anal Chem* 66:128–145.
663 <https://doi.org/10.1016/j.trac.2014.10.005>
- 664 Bicchieri M, Monti M, Piantanida G, Sodo A (2016) Effects of gamma irradiation on deteriorated
665 paper. *Radiat Phys Chem* 125:21–26. <https://doi.org/10.1016/j.radphyschem.2016.03.005>
- 666 Bouchard J, Méthot M, Jordan B (2006) The effects of ionizing radiation on the cellulose of
667 woodfree paper. *Cellulose* 13:601–610. <https://doi.org/10.1007/s10570-005-9033-0>
- 668 Burgess HD (1988) Practical Considerations for Conservation Bleaching. *JIC-CG* 13:11–26
- 669 Carter HA (1996) The Chemistry of Paper Preservation: Part 1. The Aging of Paper and
670 Conservation Techniques. *J Chem Educ* 73:417–420. <https://doi.org/10.1021/ed073p417>
- 671 Castellan A, Ruggiero R, Frollini E, et al (2007) Studies on fluorescence of cellulose.
672 *Holzforschung* 61:504–508. <https://doi.org/10.1515/HF.2007.090>
- 673 Creagh D (2007) Chapter 1 Synchrotron Radiation and its Use in Art, Archaeometry, and
674 Cultural Heritage Studies. In: *Physical Techniques in the Study of Art, Archaeology and*
675 *Cultural Heritage*. Elsevier, Amsterdam, pp 1–95
- 676 Duconseille A, Andueza D, Picard F, et al (2016) Molecular changes in gelatin aging observed by
677 NIR and fluorescence spectroscopy. *Food Hydrocoll* 61:496–503.
678 <https://doi.org/10.1016/j.foodhyd.2016.06.007>
- 679 Dupont A-L (2003a) Gelatine sizing of paper and its impact on the degradation of cellulose
680 during ageing: a study using size-exclusion chromatography. PhD thesis. Universiteit van
681 Amsterdam
- 682 Dupont A-L (2003b) Cellulose in lithium chloride/N,N-dimethylacetamide, optimisation of a
683 dissolution method using paper substrates and stability of the solutions. *Polymer*
684 44:4117–4126. [https://doi.org/10.1016/S0032-3861\(03\)00398-7](https://doi.org/10.1016/S0032-3861(03)00398-7)
- 685 Dupont A-L, Réau D, Bégin P, et al (2018) Accurate molar masses of cellulose for the
686 determination of degradation rates in complex paper samples. *Carbohydr Polym* 202:172–
687 185. <https://doi.org/10.1016/j.carbpol.2018.08.134>
- 688 Emery JA, Schroeder HA (1974) Iron-catalyzed oxidation of wood carbohydrates. *Wood Sci*
689 *Technol* 8:123–137. <https://doi.org/10.1007/BF00351367>

- 690 Ershov BG (1998) Radiation-chemical degradation of cellulose and other polysaccharides. *Russ*
691 *Chem Rev* 67:315. <https://doi.org/10.1070/RC1998v067n04ABEH000379>
- 692 Evans R, Wallis AFA (1987) Comparison of cellulose molecular weights determined by high
693 performance size exclusion chromatography and spectrometry. *Proc Fourth Int Symp*
694 *Wood Pulping Chem Paris* 1:201–206
- 695 Gervais C, Thoury M, Réguer S, et al (2015) Radiation damages during synchrotron X-ray micro-
696 analyses of Prussian blue and zinc white historic paintings: detection, mitigation and
697 integration. *Appl Phys A* 121:949–955. <https://doi.org/10.1007/s00339-015-9462-z>
- 698 Gimat A (2016) Comprehension of cellulose depolymerisation mechanisms induced by iron ions.
699 PhD thesis. Université Pierre et Marie Curie
- 700 Gimat A, Dupont A-L, Lauron-Pernot H, et al (2017) Behavior of cellobiose in iron-containing
701 solutions: towards a better understanding of the dominant mechanism of degradation of
702 cellulosic paper by iron gall inks. *Cellulose* 24:5101–5115.
703 <https://doi.org/10.1007/s10570-017-1434-3>
- 704 Gimat A, Kasneryk V, Dupont A-L, et al (2016) Investigating the DMPO-formate spin trapping
705 method for the study of paper iron gall ink corrosion. *New J Chem* 40:9098–9110.
706 <https://doi.org/10.1039/C6NJ01480A>
- 707 Gimat A, Schöder S, Thoury M, et al (2020) Short- and Long-Term Effects of X-ray Synchrotron
708 Radiation on Cotton Paper. *Biomacromolecules* 21:2795–2807.
709 <https://doi.org/10.1021/acs.biomac.0c00512>
- 710 Glaser L, Deckers D (2014) The Basics of Fast-scanning XRF Element Mapping for Iron-gall Ink
711 Palimpsests. *Manuscr Cult* 7:104–112
- 712 Henniges U, Hasani M, Potthast A, et al (2013) Electron Beam Irradiation of Cellulosic
713 Materials—Opportunities and Limitations. *Materials* 6:1584–1598.
714 <https://doi.org/10.3390/ma6051584>
- 715 IAEA (2016) Trends of Synchrotron Radiation Applications in Cultural Heritage, Forensics and
716 Materials Science. International Atomic Energy Agency, Vienna
- 717 Jeong M-J, Dupont A-L, de la Rie ER (2014) Degradation of cellulose at the wet–dry interface.
718 II. Study of oxidation reactions and effect of antioxidants. *Carbohydr Polym* 101:671–
719 683. <https://doi.org/10.1016/j.carbpol.2013.09.080>
- 720 Kabacińska Z, Yate L, Wencka M, et al (2017) Nanoscale Effects of Radiation (UV, X-ray, and
721 γ) on Calcite Surfaces: Implications for its Mechanical and Physico-Chemical Properties.
722 *J Phys Chem C* 121:13357–13369. <https://doi.org/10.1021/acs.jpcc.7b03581.s001>
- 723 Kocar D, Strlic M, Kolar J, et al (2005) Chemiluminescence from paper III: the effect of
724 superoxide anion and water. *Polym Degrad Stab* 88:407–414.
725 <https://doi.org/10.1016/j.polymdegradstab.2004.12.005>

- 726 Kozachuk M, Suda A, Ellis L, et al (2016) Possible Radiation-Induced Damage to the Molecular
727 Structure of Wooden Artifacts Due to Micro-Computed Tomography, Handheld X-Ray
728 Fluorescence, and X-Ray Photoelectron Spectroscopic Techniques. *J Conserv Mus Stud*
729 14:2–6. <https://doi.org/10.5334/jcms.126>
- 730 Mantler M, Klikovits J (2004) Analysis of art objects and other delicate samples: Is XRF really
731 nondestructive? *Powder Diffr* 19:16–19. <https://doi.org/10.1154/1.1649962>
- 732 Missori M, Righini M, Dupont A-L (2006) Gelatine sizing and discoloration: A comparative
733 study of optical spectra obtained from ancient and artificially aged modern papers. *Opt*
734 *Commun* 263:289–294. <https://doi.org/10.1016/j.optcom.2006.02.004>
- 735 Moini M, Rollman CM, Bertrand L (2014) Assessing the Impact of Synchrotron X-ray Irradiation
736 on Proteinaceous Specimens at Macro and Molecular Levels. *Anal Chem* 86:9417–9422.
737 <https://doi.org/10.1021/ac502854d>
- 738 Nevell TP (1985) Degradation of cellulose by acids, alkalis and mechanical means. Chapter 9.
739 In: Nevell TP, Zeronian SH (eds) *Cellulose chemistry and its applications*. Ellis Horwood,
740 Chichester, pp 223–242
- 741 Poggi G, Sistach MC, Marin E, et al (2016) Calcium hydroxide nanoparticles in hydroalcoholic
742 gelatin solutions (GeolNan) for the deacidification and strengthening of papers containing
743 iron gall ink. *J Cult Herit* 18:250–257. <https://doi.org/10.1016/j.culher.2015.10.005>
- 744 Potthast A, Henniges U, Banik G (2008) Iron gall ink-induced corrosion of cellulose: aging,
745 degradation and stabilization. Part 1: model paper studies. *Cellulose* 15:849–859.
746 <https://doi.org/10.1007/s10570-008-9237-1>
- 747 Pouyet E, Devine S, Grafakos T, et al (2017) Revealing the biography of a hidden medieval
748 manuscript using synchrotron and conventional imaging techniques. *Anal Chim Acta*
749 982:20–30. <https://doi.org/10.1016/j.aca.2017.06.016>
- 750 Reissland B (1999) Ink Corrosion Aqueous and Non Aqueous Treatment of Paper Objects - State
751 of the Art. *Restaurator* 20:167–180
- 752 Röhring J, Potthast A, Rosenau T, et al (2002) A Novel Method for the Determination of
753 Carbonyl Groups in Cellulosics by Fluorescence Labeling. 2. Validation and
754 Applications. *Biomacromolecules* 3:969–975. <https://doi.org/10.1021/bm020030p>
- 755 Ross-Murphy SB (1985) Properties and uses of cellulose solutions. Chapter 8. In: Nevell TP,
756 Zeronian S (eds) *Cellulose Chemistry and its Applications*. Ellis Horwood, Chichester, pp
757 202–222
- 758 Rouchon V, Belhadj O (2016) Calcium Hydrogen Carbonate (Bicarbonate) Deacidification: What
759 you always wanted to know but never dared asking. *J Pap Conserv* 17:125–127.
760 <https://doi.org/10.1080/18680860.2016.1287406>

- 761 Rouchon V, Belhadj O, Duranton M, et al (2016) Application of Arrhenius law to DP and zero-
762 span tensile strength measurements taken on iron gall ink impregnated papers: relevance
763 of artificial ageing protocols. *Appl Phys A* 122:773. [https://doi.org/10.1007/s00339-016-](https://doi.org/10.1007/s00339-016-0307-1)
764 0307-1
- 765 Rouchon V, Duranton M, Burgaud C, et al (2011) Room-Temperature Study of Iron Gall Ink
766 Impregnated Paper Degradation under Various Oxygen and Humidity Conditions: Time-
767 Dependent Monitoring by Viscosity and X-ray Absorption Near-Edge Spectrometry
768 Measurements. *Anal Chem* 83:2589–2597. <https://doi.org/10.1021/ac1029242>
- 769 Selih VS, Strlic M, Kolar J, Pihlar B (2007) The role of transition metals in oxidative degradation
770 of cellulose. *Polym Degrad Stab* 92:1476–1481.
771 <https://doi.org/10.1016/j.polymdegradstab.2007.05.006>
- 772 Sequeira S, Casanova C, Cabrita EJ (2006) Deacidification of paper using dispersions of
773 Ca(OH)₂ nanoparticles in isopropanol. Study of efficiency. *J Cult Herit* 7:264–272.
774 <https://doi.org/10.1016/j.culher.2006.04.004>
- 775 Shinotsuka H, Tanuma S, Powell CJ, Penn DR (2015) Calculations of electron inelastic mean
776 free paths. X. Data for 41 elemental solids over the 50 eV to 200 keV range with the
777 relativistic full Penn algorithm. *Surf Interface Anal* 47:1132–1132.
778 <https://doi.org/10.1002/sia.5861>
- 779 T 211 om-02 (2002) Ash in wood, pulp, paper and paperboard: combustion at 525°C. Technical
780 Association of the Pulp and Paper Industry
- 781 T 230 om-19 (1999) Viscosity of pulp (capillary viscometer method). Technical Association of
782 the Pulp and Paper Industry
- 783 T 402 sp-08 (2013) Standard conditioning and testing atmospheres for paper, board, pulp
784 handsheets, and related products. Technical Association of the Pulp and Paper Industry
- 785 T 430 cm-99 (1999) Copper Number of Pulp, Paper, and Paperboard. Technical Association of
786 the Pulp and Paper Industry
- 787 T 502 cm-07 (1998) Equilibrium relative humidity of paper and paperboard. Technical
788 Association of the Pulp and Paper Industry
- 789 T 509 om-15 (2002) Hydrogen ion concentration (pH) of paper extracts (cold extraction method).
790 Technical Association of the Pulp and Paper Industry
- 791 T 553 om-00 (2000) Alkalinity of paper as calcium carbonate (alkaline reserve of paper).
792 Technical Association of the Pulp and Paper Industry
- 793 T 573 sp-15 (2015) Accelerated temperature aging of printing and writing paper by dry oven
794 exposure apparatus. Technical Association of the Pulp and Paper Industry

- 795 Whitmore PM, Bogaard J (1994) Determination of the Cellulose Scission Route in the Hydrolytic
796 and Oxidative Degradation of Paper. *Restaurator* 15:26–45.
797 <https://doi.org/10.1515/rest.1994.15.1.26>
- 798 Yova D, Hovhannisyan V, Theodossiou T (2001) Photochemical effects and hypericin
799 photosensitized processes in collagen. *J Biomed Opt* 6:52–7.
800 <https://doi.org/10.1117/1.1331559>
- 801